# Comparison of two solvers for the extended method of fundamental solutions

R. Gospavic[1], N. Haque[1], V. Popov[1] & C. S. Chen[2]
[1]*Wessex Institute of Technology, Ashurst Lodge, Southampton, UK*
[2]*Department of Mathematics, University of Southern Mississippi, Hattiesburg, MS 39406-5045, USA*

## Abstract

In this work two solvers are compared for solution of the system of equations arising from the extended method of fundamental solutions. This method is a combination of the method of fundamental solutions (MFS) and the dual reciprocity method (DRM). The stationary and non-stationary elliptic partial differential equations with variable coefficients are considered. For the non-stationary case a finite difference time discretisation is used. Two sets of basis functions are used, a fundamental solution for the considered operator and a radial basis function (RBF) approximation for the particular solution, in particular the multiquadric (MQ) functions. A direct solver using a high number of digits and an indirect solver based on truncated singular value decomposition (TSVD) were used and compared. The method is tested for different values of the shape parameter in the MQ basis functions.

*Keywords: meshless, method of fundamental solutions, elliptic partial differential equations, non-stationary problems.*

## 1 Introduction

In recent times there has been growing interest in developing various meshless methods for the numerical solution of partial differential equations (PDEs) [1–3]. The major advantage of the meshless methods compared to the traditional numerical methods for solving PDEs is that they avoid the difficulties of meshing the domain and boundary, which is especially beneficial for 3D problems [2]. The use of meshless methods simplifies the geometrical representation of the problem domain and eliminates the need

WIT Transactions on Modelling and Simulation, Vol 47, © 2008 WIT Press
www.witpress.com, ISSN 1743-355X (on-line)
doi:10.2495/BE080191

for constructing mesh end element connectivity, instead the scattered nodes could be used without the need for connectivity [1]. The method of the fundamental solutions (MFS) uses the fundamental solution of the considered operator as the set of the basis functions for interpolation of the homogeneous solution [4–6]. To avoid the singularities the source points are placed outside of the problem domain on the fictitious boundary [7]. For the non-homogenous problem the method of the particular solutions (MPS) has been used to interpolate the non-homogeneous term by RBFs [8]. In contrast to the MPS where the homogenous particular solutions are obtained separately, in the present numerical method the particular and homogeneous solutions are combined and obtained simultaneously in one step [11, 12]. In this way the governing equations and boundary conditions are incorporated together in a single system of equations.

The two sets of basis functions are used simultaneously. The fundamental solution for the considered operator is used as the basis function for interpolation of the homogeneous solution and the MQ functions are used as RBF approximation for the particular solution [9]. For the non-stationary case the time discretization is used and the governing equation is solved by using time iterations. To obtain a high accuracy the method is tested for different values of the shape parameters. As the obtained system has a high condition number the two solvers are compared, the direct solver using a high number of digits and the TSVD solver.

## 2 The extended method of fundamental solutions (EMFS)

The following 2D time dependent boundary value problem (BVP) with appropriate boundary conditions (BC) will be considered:

$$\begin{aligned} &\Delta u(x,y,t)+\alpha(x,y)\cdot u(x,y,t)=\beta\cdot\frac{\partial u(x,y,t)}{\partial t}+f(x,y,t);\quad \vec{r}=(x,y)\in\Omega \\ &B\,u(x,y,t)=g(x,y,t);\quad \vec{r}=(x,y)\in\partial\Omega, \end{aligned} \tag{1}$$

where $\alpha(x,y)$, $f(x,y,t)$ and $g(x,y)$ are given functions, $\beta$ is a constant and $B$ is a first order operator, $\Omega$ is the 2D problem domain, and $\partial\Omega$ is the domain boundary. The non-homogeneous term could be interpreted as a source and the second term on the left side as a reactive term.

If time discretisation is performed and time derivative is approximated by finite difference the above equations could be rearranged in the following way:

$$\begin{aligned} &\Delta u(x,y,t_k)=F(x,y,u(x,y,t_k),u(x,y,t_{k-1}));\quad \Delta t=t_k-t_{k-1} \\ &F=-\alpha(x,y)\cdot u(x,y,t_k)+\beta\frac{u(x,y,t_k)-u(x,y,t_{k-1})}{\Delta t}+f(x,y,t_k), \end{aligned} \tag{2}$$

where $\Delta t$ is the time step used.

The solution in the $k$-th time step is approximated as a sum of the particular and homogenous solutions in the following way [8, 10]:

$$u^k(\vec{r},t_k)=u_h^k(\vec{r},t_k)+u_p^k(\vec{r},t_k);\quad \Delta u_h^k=0;\quad \Delta u_p^k=F(\vec{r},u^k,u^{k-1});$$
$$u_h^k\approx\sum_{j=1}^{m}b_j^k G(|\vec{r}-\vec{\rho}_j|);\quad F(\vec{r},u^k,u^{k-1})\approx\sum_{i=1}^{n}a_i^k\varphi(|\vec{r}-\vec{r}_i|);\quad G(r)=4\pi\cdot\ln(r) \tag{3}$$
$$\Delta\hat{u}(|\vec{r}-\vec{r}_i|)=\varphi(|\vec{r}-\vec{r}_i|)\Rightarrow\quad u_p^k\approx\sum_{i=1}^{n}a_i\hat{u}(|\vec{r}-\vec{r}_i|),\quad \Delta u^k\approx F(\vec{r},u^k,u^{k-1}),$$

where $\varphi(r_i)$ are RBFs used for interpolation of the non homogeneous term, $G(\rho_j)$ is a fundamental solution for the 2D Laplace operator, $u^{k-1}$ solution from previous time step, $\mathbf{r}_i$ are coordinates of the collocation points inside the domain $\Omega$, $\boldsymbol{\rho}_j$ are coordinates of the source nodes on the fictitious boundary $\Gamma$, $n$ is number of interior nodes inside $\Omega$ and $m$ is the number of nodes on the boundary $\partial\Omega$ and in the same time the number of source points on the fictitious boundary $\Gamma$, as shown in Figure 1.

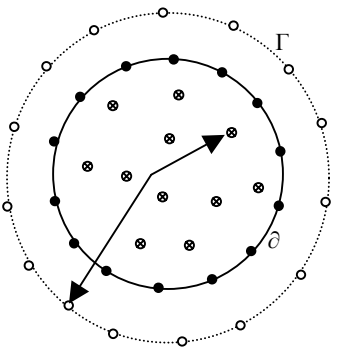


Figure 1: Arrangement of the internal, boundary and fictitious nodes.

By combining (2) and (3) the following expressions in k-th time step are obtained [8, 10]:

$$\Delta u^k=\sum_{i=1}^{n}a_i^k\Delta\hat{u}_i=\sum_{i=1}^{n}a_i^k\varphi_i=f(x,y,t^k)-\alpha(x,y)\cdot u^k+\beta\cdot\frac{u^k-u^{k-1}}{\Delta t}\Rightarrow$$
$$\sum_{i=1}^{n}a_i^k\Phi(|\vec{r}-\vec{r}_i|)+\sum_{j=1}^{n}b_j^k\Theta(|\vec{r}-\vec{\rho}_i|)\approx f(\vec{r},t^k)-\frac{\beta}{\Delta t}u^{k-1}(\vec{r}),\ \ \vec{r}=(x,y)\in\Omega \tag{4}$$

where $\Phi$ and $\Theta$ are given as:

$$\Phi(|\vec{r}-\vec{r}_i|)=\varphi(|\vec{r}-\vec{r}_i|)+\hat{u}(|\vec{r}-\vec{r}_i|)\cdot\left(\alpha(x,y)-\frac{\beta}{\Delta t}\right);$$
$$\Theta(|\vec{r}-\vec{\rho}_i|)=G(|\vec{r}-\vec{\rho}_i|)\cdot\left(\alpha(x,y)-\frac{\beta}{\Delta t}\right). \tag{5}$$

The boundary conditions in (1) are given by the following relation:

$$\sum_{i=1}^{n}a_i^k\cdot B\,\hat{u}(|\vec{r}-\vec{r}_i|)+\sum_{j=1}^{m}b_j^k\cdot B\,G(|\vec{r}-\vec{\rho}_j|)=g(x,y),\quad \vec{r}=(x,y)\in\partial\Omega \tag{6}$$

The collocation method is used and equation (4) is satisfied at $n$ interior nodes and equation (6) is satisfied at $m$ boundary nodes in each time step. In this way

the following system of linear equations of order $(n + m) \times (n + m)$ is formulated for each time step:

$$\begin{bmatrix} \Phi\left(\left|\vec{r}_i - \vec{r}_j\right|\right) & \Theta\left(\left|\vec{r}_i - \vec{r}_j\right|\right) \\ B\hat{u}\left(\left|\vec{r}_i - \vec{r}_j\right|\right) & BG\left(\left|\vec{r}_i - \vec{r}_j\right|\right) \end{bmatrix} \cdot \begin{bmatrix} \widetilde{a}^k \\ \widetilde{b}^k \end{bmatrix} = \begin{bmatrix} \widetilde{f}^k \\ \widetilde{g} \end{bmatrix};$$

$$\widetilde{a}^k = \left[a_1^k \cdots a_n^k\right], \widetilde{b}^k = \left[b_1^k \cdots b_m^k\right], \tag{7}$$

$$\widetilde{f}^k = \left[ f\left(\vec{r}_1, t^k\right) - \frac{\beta}{\Delta t} u^{k-1}\left(\vec{r}_1\right), \cdots, f\left(\vec{r}_n, t^k\right) - \frac{\beta}{\Delta t} u^{k-1}\left(\vec{r}_n\right) \right]; \quad \widetilde{g} = \left[g\left(\vec{r}_1\right), \cdots, g\left(\vec{r}_m\right)\right],$$

where $u^{k-1}(\mathbf{r}_i)$ is the solution from the $k$-1$^{th}$ time step in the interior node $\mathbf{r}_i$.

The MQ functions are used for interpolations of the non-homogeneous term and û function is expressed by the following equation [8]:

$$\hat{u}(r) = \frac{1}{9}\left(4c^2 + r^2\right) \cdot \sqrt{r^2 + c^2} - \frac{c^3}{3} \ln\left(c^2 + c \cdot \sqrt{r^2 + c^2}\right), \quad \varphi(r) = \sqrt{r^2 + c^2} \tag{8}$$

# 3 Numerical results

## 3.1 Example 1

In this example a stationary problem is considered, with non-homogeneous modified Helmholtz equation with a variable coefficient and appropriate boundary conditions of Dirichlet type, in the following form:

$$\begin{aligned} &\Delta u - x^2 y \cdot u = f(x, y); \quad (x, y) \in \Omega \\ &u(x, y) = \sin\left(y^2 + x\right) - \cos\left(y - x^2\right), \quad (x, y) \in \partial\Omega \\ &\Omega = \left\{(x, y) \middle| x \in [0,1], y \in [0,1]\right\} \end{aligned} \tag{9}$$

If the non homogeneous term is given in the following form:

$$\begin{aligned} f(x, y) = &\left(1 + x^2 \cdot (4 + y)\right) \cdot \cos\left(x^2 - y\right) + 2\cos\left(x + y^2\right) + 2\sin\left(x^2 - y\right) \\ &- \sin\left(x + y^2\right) - \left(x^2 y - 4y^2\right) \cdot \sin\left(x + y^2\right) \end{aligned} \tag{10}$$

the exact solution is given by the second equation in (9). The rectangular domain with the nodes used is shown in Figure 2.

In Table 1 the numerical results for RMSE and max error for different shape parameters $c$ obtained by using the TSVD and the direct solver as well as the condition number of the system matrix are presented

For this problem 49 interior nodes and 36 boundary and source nodes were used. The two different solvers used were: TSVD with cut off singular value equal to $10^{-13}$, and a direct solver with 100 digits precision, in this case called arbitrary precision (AP), using the *Mathematica* software. The numerical error was estimated by using the root mean square error (RMSE) at testing nodes, which were uniformly arranged over the domain, and also by using the maximal relative error in a set of testing nodes. Twenty five testing nodes, arranged uniformly over the domain in a 5×5 grid were used. The RMSE is defined as follows:

$$RMSE = \sqrt{\frac{1}{Nt} \sum_{i=1}^{Nt} \left(\widetilde{u}_i - u_i\right)^2}, \tag{11}$$

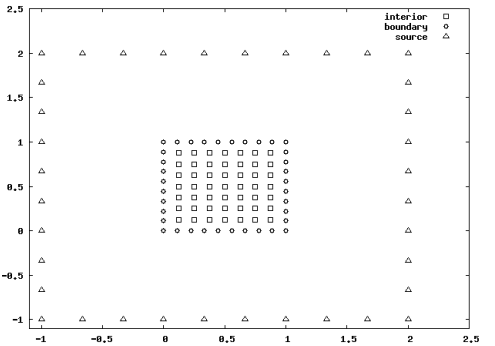


Figure 2: Problem domain with the arrangement of the interior, boundary and fictitious (source) nodes.

Table 1: Maximal relative error, RMSE and condition number of the matrix for the TSVD and the direct solver (AP).

| c | % Max Error (TSVD) | % Max Error (AP) | RMSE (TSVD) | RMSE (AP) | Condition number |
|---|---|---|---|---|---|
| 1 | 0.1418 | 0.1418 | 7.52E-006 | 2.11E-005 | 1.09E+028 |
| 2 | 0.1532 | 0.1502 | 2.75E-006 | 7.71E-006 | 2.96E+028 |
| 4 | 0.1110 | 0.0563 | 1.20E-005 | 2.58E-006 | 5.41E+029 |
| 6 | 22.676 | 0.0296 | 1.01E-003 | 1.91E-006 | 1.22E+033 |
| 8 | 482.839 | 0.0181 | 2.22E-002 | 1.90E-006 | 2.50E+036 |
| 10 | 1404.702 | 0.0133 | 5.50E-002 | 2.09E-006 | 9.21E+038 |
| 12 | 1274.686 | 0.0152 | 4.86E-002 | 2.47E-006 | 1.14E+041 |
| 14 | 7978.672 | 0.0260 | 0.27244 | 3.14E-006 | 6.73E+042 |
| 16 | 14148.345 | 0.0505 | 0.46112 | 4.32E-006 | 2.29E+044 |
| 18 | 26218.474 | 0.0961 | 1.207355 | 6.39E-006 | 5.16E+045 |
| 20 | 13318.156 | 0.1748 | 0.61568 | 9.97E-006 | 8.40E+046 |

where $Nt$ is the number of testing points, $\tilde{u}_j$ and $u_j$ are approximated and exact solutions in $j^{th}$ node, respectively.

From the above results it can be concluded that the system is ill conditioned and that the condition number of the matrix is increasing with the increase of the shape parameter, however, the precision increases as well until a certain point. It was possible to show this behaviour of the solution only when using the AP solver, the TSVD solver failed to produce accurate results for higher values of the shape parameter, showing that it is more sensitive to the value of the shape parameter $c$.

### 3.2 Example 2

The following non-stationary problem with corresponding boundary conditions was considered:

$$\begin{aligned} &\Delta u - x^2 y \cdot u = \frac{\partial u}{\partial t} + f(x,y,t); \quad (x,y) \in \Omega \\ &u = \cos(\omega t) \cdot \left(\sin\left(y^2 + x\right) - \cos\left(y - x^2\right)\right); \quad (x,y) \in \partial\Omega \end{aligned} \tag{12}$$

The problem domain and arrangement of the nodes was the same as in the previous example. If the non homogeneous term is given in the following form:

$$\begin{aligned} f(x,y,t) = {} & \omega \sin(\omega t) \cdot \left(\left(\sin\left(y^2 + x\right) - \cos\left(y - x^2\right)\right)\right) + \\ & \cos(\omega t) \cdot \left(\left(1 + x^2 \cdot (4 + y)\right) \cdot \cos\left(x^2 - y\right) + 2\cos\left(x + y^2\right)\right. \\ & \left. + 2\sin\left(x^2 - y\right) - \sin\left(x + y^2\right) - \left(x^2 y - 4y^2\right) \cdot \sin\left(x + y^2\right)\right) \end{aligned} \tag{13}$$

the exact solution is given by the second equation in (12).

In Table 2 and 3 the numerical results for maximal relative error, RMSE and the condition number for different values of the shape parameter at different time instants are presented obtained by the direct solver from *Mathematica* software, representing each number with 100 digits and by TSVD solver respectively.

Table 2: Maximal relative error, RMSE and condition number of the matrix, for the various values of the shape parameter (c) at the different time instants for the non-stationary problem obtained by the AP solver.

| C | 1 | | 5 | | 10 | | 15 | |
|---|---|---|---|---|---|---|---|---|
| Con. No. | 3.3E+14 | | 1.48E+37 | | 2.73E+37 | | 5.72E+41 | |
| Time [s] | Max rel. err % | RMSE | Max rel. err % | MSE | Max rel .err % | RMSE | Max rel err % | RMSE |
| 0 | 0.1767 | 1.76E-5 | 0.0794 | 8.47E-6 | 0.0625 | 8.39E-6 | 0.0584 | 1.14E-5 |
| 0.5 | 0.2405 | 2.27E-5 | 0.1369 | 1.26E-5 | 0.1145 | 1.25E-5 | 0.1188 | 2.04E-5 |
| 1 | 0.2407 | 2.27E-5 | 0.1375 | 1.26E-5 | 0.1149 | 1.26E-5 | 0.1199 | 2.10E-5 |
| 1.5 | 0.2408 | 2.27E-5 | 0.1377 | 1.26E-5 | 0.1149 | 1.27E-5 | 0.1200 | 2.14E-5 |
| 2 | 0.2408 | 2.27E-5 | 0.1379 | 1.27E-5 | 0.1150 | 1.29E-5 | 0.1202 | 2.19E-5 |
| 2.5 | 0.2409 | 2.27E-5 | 0.1380 | 1.27E-5 | 0.1150 | 1.31E-5 | 0.1203 | 2.26E-5 |
| 3 | 0.2410 | 2.27E-5 | 0.1381 | 1.27E-5 | 0.1151 | 1.34E-5 | 0.1204 | 2.33E-5 |
| 3.5 | 0.2410 | 2.27E-5 | 0.1382 | 1.27E-5 | 0.1151 | 1.37E-5 | 0.1205 | 2.41E-5 |
| 4 | 0.2411 | 2.27E-5 | 0.1382 | 1.27E-5 | 0.1151 | 1.42E-5 | 0.1206 | 2.50E-5 |
| 4.5 | 0.2412 | 2.27E-5 | 0.1383 | 1.27E-5 | 0.1152 | 1.49E-5 | 0.1207 | 2.60E-5 |
| 4.9 | 0.2412 | 2.27E-5 | 0.1384 | 1.27E-5 | 0.1152 | 1.57E-5 | 0.1208 | 2.68E-5 |

The maximal relative error and RMSE are calculated at the same test nodes as in the previous example.

In Figures 3 and 4 the maximal relative error and RMSE as function of the time for different shape parameters obtained by AP solver are showed respectively.

From the above results for non-stationary case the same conclusion in respect to the shape parameter is valid, as for the stationary problem in Example 1. Increasing the shape parameter decreases the error of the numerical solution but the condition number increases making the system more ill conditioned. Again a direct solver with a high number of digits should be used to obtain an accurate

Table 3: Maximal relative error, RMSE and condition number of the matrix, for the various values of the shape parameter (c) at the different time instants for the non-stationary problem obtained by the TSVD solver.

| c | 1 | | 5 | | 10 | | 15 | |
|---|---|---|---|---|---|---|---|---|
| Con. No. | 3.3E+14 | | 1.48E+37 | | 2.73E+37 | | 5.72E+41 | |
| Time | % error | RMSE | % error | RMSE | % error | RMSE | % error | RMSE |
| 0.5 | .23997 | 8.07E-6 | 1.4137 | 9.29E-5 | 8.259 | 1.40E-3 | 6485.801 | 0.2016 |
| 1 | .24044 | 8.04E-6 | 6.5621 | 2.05E-4 | 165.043 | 1.70E-2 | 9558.103 | 0.3092 |
| 1.5 | .24050 | 7.99E-6 | 2.6615 | 1.05E-4 | 90.0193 | 6.67E-3 | 13150.39 | 0.4376 |
| 2 | .24057 | 7.92E-6 | 4.7890 | 1.87E-4 | 631.892 | 1.88E-2 | 5401.139 | 0.1298 |
| 2.5 | .24064 | 7.84E-6 | 5.1626 | 1.95E-4 | 325.242 | 8.44E-3 | 33780.57 | 0.9882 |
| 3 | .24070 | 7.73E-6 | 10.422 | 2.54E-4 | 350.234 | 7.81E-3 | 4042.020 | 0.2994 |
| 3.5 | .24076 | 7.60E-6 | 6.3737 | 1.70E-4 | 1630.560 | 4.70E-2 | 56659.45 | 1.7605 |
| 4 | .24083 | 7.45E-6 | 6.5225 | 1.72E-4 | 534.308 | 1.19E-2 | 47882.97 | 1.3022 |
| 4.5 | .24091 | 7.29E-6 | 8.1751 | 2.20E-4 | 1440.991 | 3.90E-2 | 53565.09 | 1.6180 |
| 4.9 | .24095 | 7.14E-6 | 8.2750 | 1.75E-4 | 795.872 | 2.73E-2 | 83151.63 | 2.3197 |

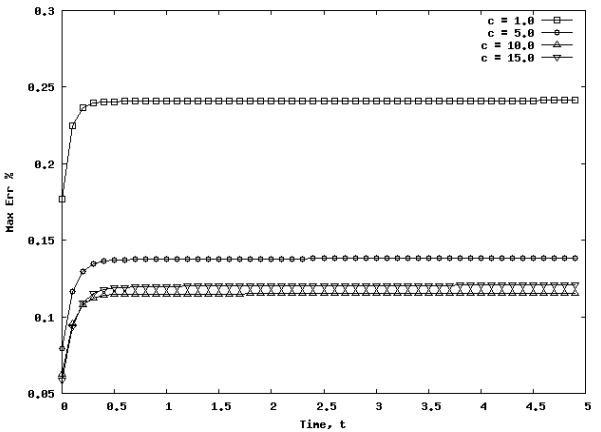


Figure 3: Maximal relative error versus time for different values of the shape parameter for results obtained using the AP direct solver.

solution that is less sensitive to the value of the shape parameter in the MQ function. In both cases the best results are obtained for shape parameter equal to 10.

## 4 Conclusions

A comparison is presented of results obtained using two different solvers with the meshless approach based on the method of particular solutions and the method of fundamental solutions. The stationary and non-stationary elliptic PDE is considered and a good agreement with the analytical solution is obtained, even

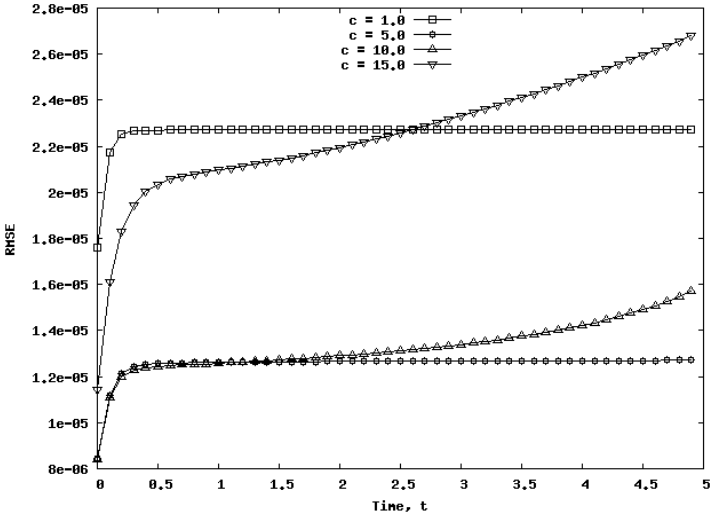


Figure 4: RMSE versus time for different values of the shape parameter for results obtained using the AP direct solver

for small numbers of interior and boundary nodes. In order to avoid singularities the source nodes for fundamental solutions are arranged outside the domain on a fictitious boundary. For approximation of the particular solutions MQ functions are applied. The accuracy of the method increases with the increase of the shape parameter, however, the condition number increases as well. The direct solver with a high number of digits, in this case 100 digits, was used in order to overcome the ill conditioning of the system matrix. An indirect solver based on the TSVD failed to solve the system for higher values of the shape parameter, showing higher sensitivity than the direct solver to the selection of the shape parameter. This results show that in some cases a large number of digits must be used in the solution of the system arising from this numerical approach.

## References

[1] Jichun Li, Y.C. Hon, C.S. Chen, Numerical comparisons of two mesh less methods using radial basis functions, Engineering Analysis with Boundary Elements **26** (2002) 205–225.

[2] C.-S. Huang, C.-F. Lee, A.H.-D. Cheng, Error estimate, optimal shape factor, and high precision computation of multiquadric collocation method, Engineering Analysis with Boundary Elements **31** (2007) 614–623.

[3] M.A. Golberg, C.S. Chen, The method of fundamental solutions for potential, Helmholtz and diffusion problems. In: M.A. Golberg, editor. Boundary integral methods-numerical and mathematical aspects. Southampton: Computational Mechanics Publications; 1998. p. 102–76.

[4] Graeme Fairweather, Andreas Karageorghis, P.A. Martin, The method of fundamental solutions for scattering and radiation problems, Engineering Analysis with Boundary Elements **27** (2003) 759–769.
[5] G. Fairweather, A. Karageorgis, The method of fundamental solution for elliptic boundary value problems, Advances in Computational Mathematics, **9**, 69–95.
[6] C.S. Chen, Hokwon A. Cho, M.A. Golberg, Some comments on the ill-conditioning of the method of fundamental solutions, Engineering Analysis with Boundary Elements **30** (2006) 405–410.
[7] P.W. Patridge, B. Sensale, The method of fundamental solutions with dual reciprocity for diffusion and diffusion-convection using subdomains, Engineering Analysis with Boundary Elements **24** (2000) 633–641
[8] M.A. Golberg, C.S. Chen, Discrete Projection Methods for Integral Equations, Computational Mechanics Publications, Southampton.
[9] M.D. Buhmann, Radial basis functions: theory and implementations, University Press, Cambridge, 2003.
[10] P.W. Partridge, C.A. Brebbia, L.C. Wrobel The Dual Reciprocity Boundary Element Method. Computational Mechanics Publications, (1992), London
[11] C.S. Chen, C. M. Fan and J. Monroe, The method of fundamental solutions for solving elliptic partial differential equations with variable coefficients, submitted.
[12] H. Wang and Q.H. Qin A meshless method for generalized linear or nonlinear Poisson-type problems, Engineering Analysis with Boundary Elements, 30, 515–521, 2006.